Supplementary Information for

Flexible depth-of-focus, depth-invariant resolution photoacoustic microscopy with Airy beam

This is a supplemental material that contains the following details that we could not include in the main paper due to space restrictions, including four Suppl Notes listed below.

TABLE OF CONTENTS

Supplementary Note 1:

1. Simulation comparison between Gaussian and Airy beam

By considering the 2D finite-energy exponentially truncated Airy function as the Fourier transform of a Gaussian beam modulated by a cubic spatial phase, we can determine the representative wave in the Fourier space (or normalized k-space) as $\phi(k) = exp(-ak^2)\, exp(\frac{i}{3}(k^3 - 3a^2k - ia^3))$ [25, 32, 33]. Based on this analysis, we generate the phase pattern for programming the design. The simulation results depicting the intensity distribution and propagation properties of both the Gaussian and Airy beams are present in Figs. S1(a) and S1(b), respectively. The results clearly demonstrate that the focus spot of the Airy beam at the focal position is smaller compared to the Gaussian beam. Additionally, the Gaussian beam diverges faster than the Airy beam when at the same distance from the focus. Moreover, from the beam propagation distance diagram at the bottom of Figs. S1(a) and S1(b), it is evident that the Airy beam exhibits a longer DOF compared to the Gaussian beam. The positions of the white dashed lines correspond to cross-sections of the two beams (I, II), respectively. Analyzing the xy-direction cross section and xz-direction depth propagation diagram of the beam, it becomes apparent that the Airy beam possesses better focusing properties (spot size) and the ability to extend the focal length compared to the Gaussian beam. From these observations, we can infer that photoacoustic microscopy (PAM) utilizing Airy beam excitation has the potential to significantly extend the DOF while maintaining relatively ideal resolution.

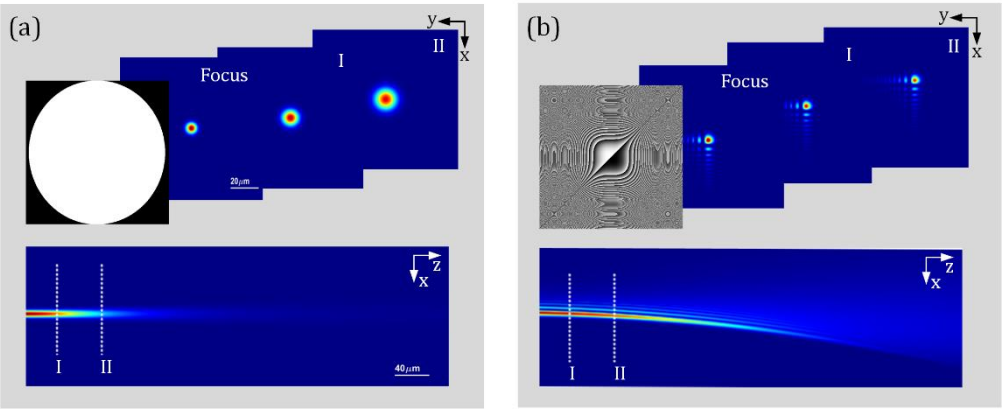

Fig. S1. The simulation results of Gaussian beam and Airy beam for property analysis. (a) Phase pattern of Gaussian beam, focus position and defocus position section maps, and xz direction propagation property maps. The cross-section maps of I and II in xy direction correspond to the dotted line of xz direction maps. (b) Airy beam phase pattern, focus position and defocus position section maps, and xz direction propagation property maps. The cross-section maps of I and II in xy direction correspond to the dotted line of xz direction maps.

Supplementary Note 2:

2. Simulation experiments of Side-lobe suppressed Airy beams

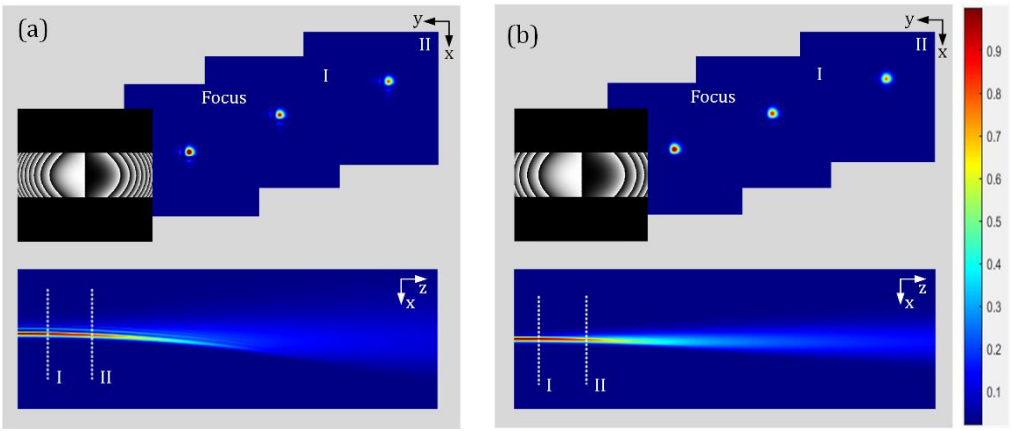

Fig. S2. The simulation results of sidelobe-suppressed Airy beam for property analysis. (a) Sidelobe-suppressed Airy beam phase pattern (a=0.2), focus position and defocus position section maps, and xz direction propagation property maps. The cross-section maps of I and II in xy direction correspond to the dotted line of xz direction maps. (b) Sidelobe-suppressed Airy beam phase pattern (a=0.4), focus position and defocus position section maps, and xz direction propagation property maps. The cross-section maps of I and II in xy direction correspond to the dotted line of xz direction maps.

In order to further optimize the beam quality, the influence of side-lobe on imaging quality is eliminated. We designed the phase modulation maps of weakening sidelobe [30], and the corresponding simulation experiment results of Airy beam with different modulation parameters are present in Fig. S2. Note that the decay factor of Fig. S2(a) is larger than that of Fig. S2(b). As can be seen from the xy section maps, the sidelobe of Airy spot at the focus position and defocus position is significantly weakened, while the main lobe spot is not affected and still maintains a good intensity distribution. Furthermore, as can be seen from the bottom xz maps, the Airy beam shows a good DOF in the propagation direction, and the main lobe is also well weakened. The above results show that we can further obtain the ideal modulation results of Airy beam by modifying the cubic phase pattern to avoid the influence of sidelobe on microscopic imaging.

Supplementary Note 3:

3. Comparison of Gaussian and Side-lobe suppressed Airy beams PAM

Figure S3 gave the comparisons among Gaussian-, Airy-beam excitation, and sidelobe-suppressed PAM imaging results. Prior to imaging, the phase pattern of the Airy beam was processed by an additional grating, separating the zeroth (unmodulated) and first order (desired) of diffraction. The image sample was a patterned copy of the letter “XDU”, which were immobilized in a solution containing a mixture of 1.6% Intralipid and 1% agar gel and tilted down at an angle to ensure a height difference of more than 2 mm. The imaging region of interest is 6 mm ×10 mm and the step size is 10 microns. Figure S3 (a) showed the imaging results of Gaussian-, Airy-beam excitation, and sidelobe-suppressed PAM, respectively. The further comparisons demonstrating the DOF and artifact condition were present from three close-up region of interest (b)-(d), corresponding to (I)-(III) in (a). In Fig. S3 (b), it can be observed

from the imaging results that PAM excited by Gaussian beam possesses obvious fuzzy areas and some details are missing. Compared with Gaussian-beam excitation PAM, Airy beam-excitation PAM showed improved DOF, however, the artifact can still be identified. In contrast, sidelobe-suppressed Airy PAM has superior imaging quality, including uniform high-resolution, detail retention of large depth-of-field, and no significant sidelobe artifacts. Compared to Gaussian- and Airy-beam excitation PAM, more clearly detailed observation from Figs. S3 (c) and S3 (d) showed that the depth-of-field extension and artifact suppression ability can be further achieved by side-suppressed Airy PAM (white arrows regions). The results show that we can further optimize the microscopic imaging quality by modifying the phase pattern of Airy beam, which has potential applications in high-resolution characterization of microcirculation pathophysiology and other related diseases.

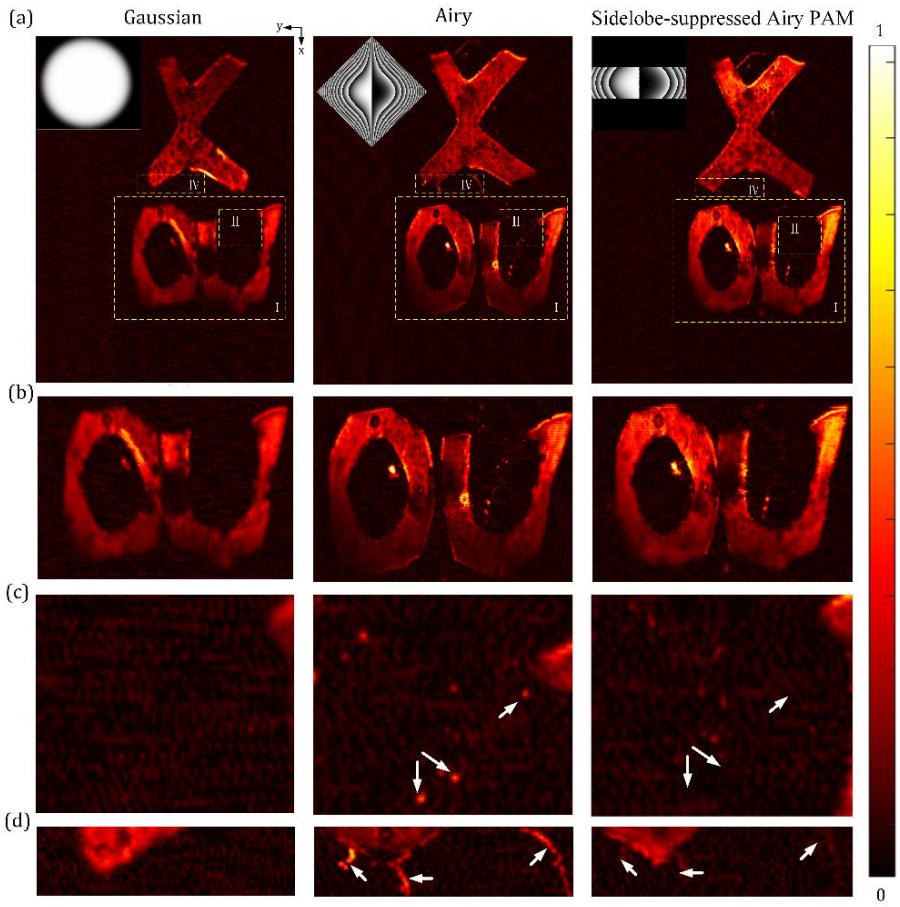

Fig. S3. Comparison of Gaussian-, Airy-beam excitation, and sidelobe-suppressed PAM in phantom experiment. Left: Imaging result of Gaussian-beam excitation PAM. Middle: Imaging result of Airy-beam excitation PAM. Right: Imaging result of sidelobe-suppressed Airy PAM.